THE AMERICAN MINERALOGIST, VOL. 55, JULY–AUGUST, 1970

HEMIHEDRITE, A NEW MINERAL FROM ARIZONA

SIDNEY A. WILLIAMS, *Western Exploration Office, Phelps Dodge Corporation, Douglas, Arizona 85607*;

JOHN W. ANTHONY, *Department of Geology, University of Arizona, Tucson, Arizona 85721.*

ABSTRACT

Hemihedrite is a new species discovered at the Florence Lead-Silver mine in Pinal County, Arizona. A second locality is the Rat Tail claim near Wickenburg, Maricopa County, Arizona.

Hemihedrite is named in allusion to its morphology. Crystals exhibit triclinic hemihedral symmetry with $\alpha=120°01'$, $\beta=91°40'$, $\gamma=55°55'$, $a:b:c=0.8345:1:0.9360$. Three twin laws have been found. The refringence is $\alpha=2.105$, $\beta=2.32$, $\gamma=2.65$(25°C); optically (+) with $2V$(calc.) $=88°$. Dispersion is strong and unsymmetric.

Crystals are orange to almost black and have a saffron yellow streak. Hardness on the Mohs scale is 3.

Unit-cell data at 22°C are as follows: $P1$; $a=9.497\pm.001$Å, $b=11.443\pm.002$ Å, $c=10.841\pm.002$ Å; $\alpha=120°30'$, $\beta=92°06'$, $\gamma=55°50'$. The Delaunay cell is $a'=9.954$ Å, $b'=10.841$ Å, $c'=9.497$ Å; $\alpha'=92°06'$, $\beta=107°58'$, $\gamma_1=123°16'$. The most intense X-ray lines are: 4.872 (90) (120), 4.364 (80) (220), 3.301 (100) $(1\bar{2}2)$, 3.146 (80) (320), 3.102 (80) (103, 102), 2.924 (55) $(2\bar{3}3)$, 2.849 (45) $(\bar{2}\bar{4}2)$, 2.182 (45b) (411, 340). $\gamma'=123°16'$. Transformation (morphology to Delaunay cell) is $\bar{1}10/001/100$.

Chemical analyses combined with structural information lead to the composition $ZnF_2[Pb_5(CrO_4)_3SiO_4]_2$(with $Z=1$), although chemical compositional variation is indicated. Specific gravity is 6.42 (meas. at 24.2°C) and the density (calc.) is 6.50 g/cm³.

Hemihedrite forms in the oxide zone of lead-bearing veins. Associated minerals may include the following: cerussite, phoenicochroite, vauquelinite, willemite, and wulfenite.

INTRODUCTION

Specimens of the new mineral were first collected and submitted to us by R. W. Thomssen. The specimens were found at the Florence Lead-Silver mine in the Tortilla mountains, Pinal County, Arizona. Subsequent trips to the locality yielded ample material for this investigation. During the study a second locality was discovered on the Rat Tail claim (formerly the Pack Rat claim) near Wickenburg, Maricopa County, Arizona. Material from the type locality in Pinal County was used as a basis for this investigation. At both localities the species is rather abundant. The species is named in allusion to its distinctive morphology.[1]

GEOLOGY

At the Florence Lead-Silver mine an adit has been driven along a strong fault zone striking N 70° E and dipping 70° to 77° to the southeast.

---

[1] The mineral and name have been approved by the Commission of New Minerals and Mineral Names, IMA.

Lead minerals including hemihedrite and wulfenite are concentrated in a shoot of small horizontal dimensions localized within the sheared and mineralized rubble and gouge in the hanging wall of the fault. Where the lead minerals occur, a crosscut has been driven exposing the fault zone and hanging wall rocks. The zone consists of nine feet of calcite and associated iron oxides cementing partly altered and replaced fragments of quartzite, limestone, and latite porphyry. Remnant galena occurs as replacements of siliceous fragments adjacent to the fault plane near the footwall side of the zone.

Supergene alteration of the calcite and galena has been most intense on the north side of the fault zone in a narrow selvage which consists of a loose aggregate of finely crushed and highly altered rock fragments and iron oxides. Secondary lead minerals occur as oxidation products in cavities left by the leaching of galena, on fractures traversing the fault-zone rubble, and in the aforementioned highly altered selvage.

Strongly brecciated Mississippian Escabrosa Limestone, intruded by altered latite porphyry, comprises the south wall of the mineralized zone. Large displacement on the northeast fault has brought these hanging wall rocks against a footwall section composed of vertically-dipping Precambrian Troy Quartzite and underlying units of the Mescal Limestone. A dike of altered diabase separates the Troy Quartzite and the uppermost chertstone unit of the Mescal Limestone on the surface over the adit. Underground the diabase has been displaced by a small fault and is not visible.

OCCURRENCE

Hemihedrite occurs in an oxide assemblage indicative of alkaline solutions of relatively low Eh (Williams, 1966). Primary minerals from which the oxide assemblage is derived consisted of galena, sphalerite, pyrite, and minor tennantite. Chalcopyrite occurs very sparingly as blebs in the sphalerite. Chromates occur where the oxide ores are near an altered diabase dike; one sample of this dike showed a CrO_3 content of 0.14 weight percent by X-ray fluorescence analysis.

Oxidation of the sulfide ores has been almost complete so that only minor amounts of galena remain in an oxide assemblage consisting largely of hemihedrite, wulfenite, willemite, and cerussite. Other species noted are vauquelinite, minium, and mimetite.

The paragenesis in the oxide asemblage is as follows: cerussite (first) followed by hemihedrite and wulfenite, with wulfenite continuing to crystallize after hemihedrite, and vauquelinite (last). Willemite is evidently earlier and mimetite is later than most wulfenite. Wulfenite contemporaneous with hemihedrite is orange and chrome-free. Wulfenite which has replaced hemihedrite is brilliant red and contains, in one analyzed specimen, 0.83 weight percent CrO_3. Continued crystallization of later wulfenite was marked by continuously decreasing chrome content; late wulfenite is yellow and chrome-free.

At the Rat Tail claim hemihedrite occurs in a similar assemblage which consists largely of hemihedrite, willemite, cerussite, and phoenicochroite, with minor amounts of mimetite and vauquelinite. These minerals have formed by oxidation of galena, sphalerite, and pyrite in quartz veins which cut an andesite agglomerate.

PHYSICAL PROPERTIES

Crystals of hemihedrite range in color from bright orange to henna brown to almost black. Crystals vary in length from 0.2 to 10 mm, and average 0.5 mm. The streak is saffron yellow (Munsell 5Y 8/10). Hardness on the Mohs scale is 3. The specific gravity measured on the Berman density balance is 6.42 (24.2°C).

CHEMICAL COMPOSITION

The initial qualitative spectrographic examination of hemihedrite showed major Pb, Cr, and Zn; traces of Ca, Si, Mg, Cu, Ni, Ag, and Al; and failed to show F. Several quantitative analyses were made by different methods for Pb, Cr, and Zn. One of these analyses showed significant Ca and a second showed significant Si. The infrared spectrum failed to reveal either water or hydroxyl, but did confirm chromate ion. A thermogravimetric balance tracing showed no weight loss to 313°C, then a gradual loss amounting to 10.7 percent of the initial weight between 313°C and 967°C. The crystal-structure analysis (McLean and Anthony, 1970) indicated two sites that would be most logically filled by Si in the one instance and F in the other, based on scattering power, charge, and atom size. Subsequent chemical work verified their presence. Electron-microprobe examination of hemihedrite established that the silicon is uniformly distributed throughout the mineral and not present in a separate phase. Table 1 presents the analytical results.

The empirical composition derived from the average analysis (column 14, Table 1) by assuming six CrO_3 per unit cell as indicated by the structure and the consistency of the Cr analyses is:

$$Zn_{1.37}F_{8.25}[Pb_{4.86}(CrO_4)_3(SiO_4)_{0.83}]_2.$$

The ideal formula deduced from the crystal structure is:

$$ZnF_2[Pb_5(CrO_4)_3SiO_4]_2.$$

The excess Zn and deficiency of Pb in the analyses are presumably due

TABLE 1. CHEMICAL ANALYSES OF HEMIHEDRITE.

	1	2	3	4	5	6	7	8	9	10	11	12	13	14	15	16		17
ZnO	Major	5.39	5.13	2.0	4.4	2.81	2.76							3.93	3.93	.046	1.37	2.7
CaO	Trace			1.1	0.0													
PbO	Major	72.82	72.15	72.7	73.3									72.74	70.5	.326	9.71	73.0
CrO_3	Major	20.00	19.95	20.6	20.0									20.14	19.5	.201	6.00	19.7
SiO_2	Trace				3.3			5.94	3.21	2.0	2.1			3.31	3.2	.056	1.66	3.9
F	Nil											4.6	5.9	5.25	5.1	.277	8.25	1.2
Totals		98.21	97.23	96.4	100.0									105.40	102.1			100.5
												$-0 \equiv F$		−2.20	−2.1			−.5
														103.17	100.0			100.0

1. Emission spectrum.
2. Atomic absorption, Hawley and Hawley, Assayers and Chemists, Tucson.
3. X-ray fluorescence.
4. Atomic absorption, George Roseveare, Arizona Bureau of Mines.
5. Quantitative chemical, Jun Ito; corrected for $PbMoO_4$ and $PbCO_3$ impurities, calibrated to 20.2% CrO_3, and recalculated to 100%.
6. Atomic absorption.
7. Atomic absorption.
8. Electron probe, R. Laughon, NASA, Manned Spacecraft Center, Houston.
9. Electron probe, R. W. Thomssen, U. S. Natural Museum and University of Arizona. F not detected by microprobe. Lower limit of detectability about 1.5 weight percent.
10. Colorimetry.
11. Colorimetry.
12. Colorimetry, G. E. Draper, Agricultural Experiment Station, University of Arizona.
13. Colorimetry, G. E. Draper.
14. Average of all analyses with Ca combined with Zn.
15. Average recalculated to 100%.
16. Mole ratios.
17. $ZnF_2[Pb_5(CrO_4)_3SiO_4]_2$.

to substitution of Zn for Pb in some samples. Fluorine in the amount indicated by the colorimetric analyses is inconsistent with the evidence from the structure and with the charge requirements of the remainder of the compound. The addition of both SiO_2 and F in the amounts indicated by the analyses made subsequent to the analyses 2–4 of Table 1 would result in totals consistently greater than 100 percent (average 103.6), while addition of fluorine in the amount indicated by the structure analysis would give totals much closer to 100 percent (average 101.2) in all cases. Therefore, we believe the fluorine analyses to be too high.

The results of the refined X-ray structure analysis ($R=4$ percent) (McLean and Anthony, 1970) lead us to the ideal composition $ZnF_2[Pb_5(CrO_4)_3SiO_4]_2$, but the variability in the analyses indicates that some compositional variation does exist. There is, however, insufficient chemical evidence to justify proposing a specific formula to express the compositional variation for the species.

Reactions of hemihedrite to certain reagents are as follows: in 1:1 HNO_3, white powdery $Pb(NO_3)_2$ is formed; in 1:1 HCl, a coating of $PbCl_2$ slowly develops. Hemihedrite is slowly decomposed in 20 percent KOH, but is unaffected by 20 percent NH_4OH.

MORPHOLOGY

Hemihedrite crystals of great perfection and ideal size for goniometry were easily obtained. About 40 crystals were measured on a Stoe two-circle goniometer. Many of these were doubly terminated. About a dozen twins were also examined. The morphological study shows that the crystals are triclinic hemihedral. Goniometric data for a single crystal and three twins are given in Table 2. Similar results for many crystals were averaged (using only faces regarded as good or excellent) to calculate the crystallographic elements from which the angle table (Table 3) is derived.

The angle table is for a right-handed crystal; left-handed crystals show all the complementary forms. A complete list of forms is given here:

vertical: $b\{010\}$, $\bar{b}\{0\bar{1}0\}$, $a\{100\}$, $\bar{a}\{\bar{1}00\}$, $\{120\}$, $m\{110\}$, $\{310\}$, $\{\bar{1}\bar{2}0\}$, $\{\bar{2}\bar{3}0\}$, $\{\bar{3}\bar{4}0\}$, $\bar{m}\{\bar{1}\bar{1}0\}$, $\{\bar{3}\bar{2}0\}$, $\bar{w}\{\bar{2}\bar{1}0\}$, $\{\bar{3}\bar{1}0\}$, $M\{1\bar{1}0\}$, $\{\bar{1}20\}$, and $\bar{M}\{\bar{1}\bar{1}0\}$.

upper: $c\{001\}$, $d\{0\bar{1}2\}$, $p\{0\bar{1}1\}$, $\{0\bar{3}2\}$, $q\{0\bar{2}1\}$, $\{102\}$, $\{203\}$, $h\{101\}$, $t\{\bar{1}01\}$, $\{\bar{4}03\}$, $\{112\}$, $r\{111\}$, $u\{1\bar{1}2\}$, $f\{1\bar{1}1\}$, $\{\bar{1}14\}$, $s\{\bar{1}11\}$, $S\{\bar{1}\bar{1}1\}$, $\{122\}$, $x\{\bar{2}12\}$, $\{\bar{1}\bar{2}1\}$, $\{\bar{3}\bar{5}5\}$, $\{\bar{1}\bar{3}1\}$, $\{\bar{6}\bar{1}4\}$, $\{\bar{3}\bar{2}2\}$, $\{\bar{3}\bar{4}2\}$, $\{\bar{3}\bar{5}2\}$, $\{\bar{5}\bar{3}3\}$, and $\{\bar{5}\bar{3}2\}$.

lower: $\bar{c}\{00\bar{1}\}$, $\bar{d}\{01\bar{2}\}$, $\{03\bar{4}\}$, $\bar{p}\{01\bar{1}\}$, $\{03\bar{2}\}$, $\bar{q}\{02\bar{1}\}$, $\{10\bar{2}\}$, $\bar{h}\{\bar{1}0\bar{1}\}$, $\bar{l}\{10\bar{1}\}$, $\{20\bar{1}\}$, $\{\bar{1}0\bar{2}\}$, $\{11\bar{6}\}$, $\{11\bar{3}\}$, $\{11\bar{2}\}$, $\bar{S}\{11\bar{1}\}$, $\bar{s}\{1\bar{1}\bar{1}\}$, $\bar{u}\{\bar{1}1\bar{2}\}$, $\bar{f}\{\bar{1}1\bar{1}\}$, $\bar{r}\{\bar{1}\bar{1}\bar{1}\}$, $\{12\bar{2}\}$, $\{12\bar{1}\}$, $\{13\bar{1}\}$, $\{92\bar{6}\}$, $\{31\bar{2}\}$, $\{32\bar{2}\}$, $\{21\bar{1}\}$, $\{23\bar{1}\}$, $\{32\bar{1}\}$, $\{21\bar{2}\}$, $\bar{x}\{2\bar{1}\bar{2}\}$, $\{\bar{4}3\bar{6}\}$, $\{\bar{2}\bar{1}4\}$, and $\{\bar{3}\bar{2}6\}$.

TABLE 2. TYPICAL GONIOMETRIC DATA[a]

Single Crystal			Twin on ($0\bar{1}2$)		
Face	V	H	Face	V	H
010	349°10′	90°00′	010	16°16′	90°00′
$\bar{1}00$	40 06	90 00	*010*	16 18	91 07
$\bar{1}\bar{1}0$	103 00	90 00	110	83 07	90 00
$0\bar{1}0$	169 08	90 00	*210*	83 08	93 02
100	220 08	90 00	100	145 26	90 00
$\bar{1}1\bar{1}$	25 14	63 25	*100*	145 28	92 01
$02\bar{1}$	350 09	64 43	$\bar{2}12$	350 54	69 11
$11\bar{1}$	247 06	48 40	$0\bar{2}1$	195 25	64 59
$01\bar{1}$	351 51	34 36	111	60 30	59 30
$\bar{1}1\bar{2}$	42 57	36 45	001	18 33	35 44
$00\bar{1}$	166 36	35 57	$\mathit{\bar{2}12}$	350 15	110 46
$01\bar{2}$	112 33	2 06	$\mathit{0\bar{2}1}$	195 28	114 54
			111	60 21	123 18
Twin on ($\bar{2}\bar{2}3$)			Twin on ($0\bar{1}0$)		
110	232°39′	90°00′	010	82°29′	90°00
$\bar{2}\bar{1}0$	0 45	90 00	*100*	133 30	90 00
$\bar{1}00$	23 30	90 00	100	211 32	90 00
010	75 31	90 00	*010*	262 30	90 00
100	204 18	90 00	$\bar{2}12$	57 08	69 09
$0\bar{1}0$	255 02	88 07	$\mathit{\bar{2}12}$	287 50	69 08
$0\bar{2}1$	252 37	65 12	$0\bar{2}1$	261 50	64 59
$\mathit{0\bar{2}1}$	252 37	65 12	$\mathit{0\bar{2}1}$	83 17	65 03
$\mathit{0\bar{1}0}$	279 31	58 39	111	126 43	59 30
$\mathit{0\bar{1}1}$	223 50	78 50	001	84 45	35 43
$\mathit{0\bar{1}2}$	194 02	97 32	*001*	260 12	35 50
001	161 57	113 55	$0\bar{1}2$	164 10	1 41
$1\bar{1}1$	218 07	65 03	$\mathit{0\bar{1}2}$	180 50	1 40
$\bar{1}\bar{1}1$	357 58	46 12			
001	81 21	36 12			
$0\bar{1}2$	148 16	4 43			
010	100 30	121 20			
100	253 55	11 48			

[a] Italicized indices are underlined in Figures 3–6.

The major forms are *c*, $\bar{c}$, *a*, $\bar{a}$, *b*, *m*, $\bar{p}$, *q*, $\bar{q}$, *t*, *d*, and *f*. Various habits are illustrated in Figure 1.

The morphological setting makes the best zone the *c* axis. This zone, dominated by *a*, $\bar{a}$, *m*, $\bar{m}$, and *b*, is one of moderate elongation. Another strong zone, used for the *a* axis, includes *c* and *q*; *c* is the brightest and most persistent face close to a polar position. Other orientations were tried but none gave as low a sum of indices as that adopted.

Evidence for hemihedrism is excellent. Many crystals show a large bright *c* and a small etched $\bar{c}$; a large, smooth *b* and small, etched, or

TABLE 3. CALCULATED ANGLES FOR HEMIHEDRITE.

$a:b:c=0.8345:1:0.9630$ $\alpha=120°01'$ $\beta=91°40'$
$\gamma=55°55'$ $\lambda=54°14'$ $\mu=110°30'$ $\nu=129°06'$
$x_0'=.0292$ $y_0'=.7208$ $p_0'=1.4876$ $q_0'=1.4311$
$p_0:q_0:r_0=1.2064:1.1622:1$

Forms		ϕ	ρ	A	B	C
Lower	Upper & Vertical					
	c 001	2°18′	35°48′	110°30′	54°14′	0°00′
$\bar{c}$ $00\bar{1}$		−177 42	144 12	69 30	125 46	180 00
	b 010	0 00	90 00	129 06	0 00	54 14
	$\bar{b}$ $0\bar{1}0$	180 00	90 00	50 54	180 00	125 46
	a 100	129 06	90 00	0 00	129 06	110 30
	$\bar{a}$ $\bar{1}00$	−50 54	90 00	180 00	50 54	69 30
	m 110	66 48	90 00	62 18	66 48	75 24
	M $1\bar{1}0$	154 02	90 00	24 56	154 02	121 01
$\bar{p}$ $01\bar{1}$		−2 20	144 31	112 35	54 33	108 46
	q $0\bar{2}1$	179 14	65 00	54 28	155 00	100 46
$\bar{q}$ $02\bar{1}$		0 46	115 00	125 32	25 00	79 14
	h 101	100 24	50 16	47 34	97 59	62 56
	f $1\bar{1}1$	144 22	63 47	30 04	136 48	93 12

Direct and reciprocal matrices of Bond (1946) and Evans (1948):

$$M=\begin{Vmatrix} .83415 & .54608 & 0 \\ 0 & .67142 & 0 \\ .02427 & .50025 & .9630 \end{Vmatrix}$$

$$M^{-1}=\begin{Vmatrix} 1.1988 & -.97503 & 0 \\ 0 & 1.4894 & 0 \\ -.03022 & -.74347 & 1.0384 \end{Vmatrix}$$

absent $\bar{b}$; large and deeply etched M while $\overline{M}$ is small, vicinal, and unetched. Etching in 10 percent $FeCl_3$ was especially successful on m and $\bar{m}$, m etched deeply while $\bar{m}$ was but slightly affected; etch patterns for these two forms are quite different. Both right- and left-handed crystals show preferential etching of m. In 1:5 HCl, m corrodes very rapidly and becomes coated with powdery $PbCl_2$ while $\bar{m}$ is notably less affected. Similar preferential corrosion was noted in dilute HNO_3.

Commonly the crystals have a large blunt positive end and a small tapered negative end. Choice of the blunt end as positive obeys convention for polar species.

Visual examination of many crystals indicates that about 75 percent are right-handed and that the negative ends of crystals of both hands point away from the matrix about 90 percent of the time. Overall devel-

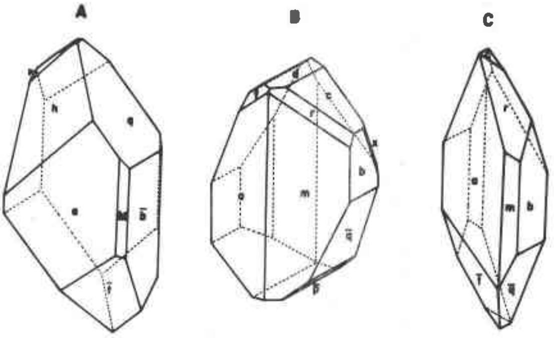

Fig. 1. A, left-handed crystal. + end up; B and C, right-handed crystals, + ends up.

opment of the crystals and especially the appearance of *c* and *b* were used to determine the handedness and sign of the *c* axis.

The preceding discussion applies to material from the type locality. Crystals from the Rat Tail claim show almost identical habit and forms. No twins were observed in the Rat Tail material but several laws are recognized in the type material.

The most common type of twinning is twinning by reflection in $(\overline{2}\overline{2}3)$. These crystals occur as penetrations of individuals of opposite hand which form an *X*, *V*, or *Y* with their *c* axes inclined at about 102°. The faces (021) are exactly parallel in the two individuals and often are abnormally large. About 50 of these twins were observed. They tend to be common in certain vugs rather than systematically distributed throughout the material. These twins are shown in Figure 2, C and D.

A less common type of twinning is twinning by reflection in $(0\overline{1}0)$. Normally the composition surface is (010) (Figure 2-B), but on occasion it may follow the base of terminal forms. Some of these twins which show no reentrant simulate monoclinic class *m* symmetry.

A third law (Figure 2-A) involves two individuals twinned by reflection in $(0\overline{1}2)$ which is a pseudo-monoclinic *b* face. A number of these twins were found on one specimen.

Stereographic projections of a single crystal and examples of measured twins are shown in Figures 3 through 6.

X-RAY DIFFRACTION STUDY

The morphological orientation was retained in selecting the unit cell of hemihedrite. Rotation and Weissenberg photographs were made around each of the three morphological axes. Evidences of the point-group symmetry considered under the discussion on morphology show the space group to be *P*1.

Unit-cell constants were derived independently from data collected by

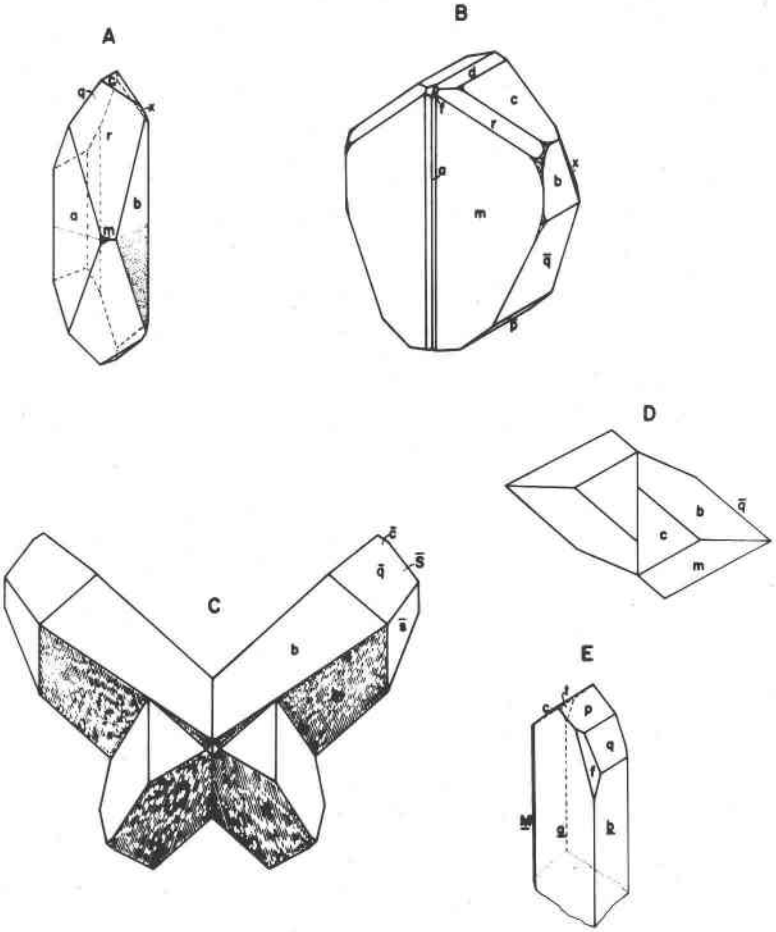

Fig. 2. A, twin on (0$\bar{1}$2); B and E, twin on (0$\bar{1}$0); C and D, twin on ($\bar{2}\bar{2}$3).

the Weissenberg method and with a Picker single crystal diffractometer.[1] In both cases reflections were measured from spheres about 0.05 mm in diameter ground from single, untwinned crystals, Wiessenberg-film calibration was made with sodium chloride powder ($a_0 = 5.6402$ Å) at 22°C. 2θ angles from 108 reflections were used to calculate and refine the cell constants through a least squares routine with a program written for the IBM 1620 computer. Exdellent agreement was obtained between these parameters and those derived from the diffractometer measurements of 29 reflections similarly processed. Table 4 gives the cell con-

---

[1] The refined cell constants were determined by Dr. W. John McLean at the Crystallography Laboratory, University of Pittsburgh.

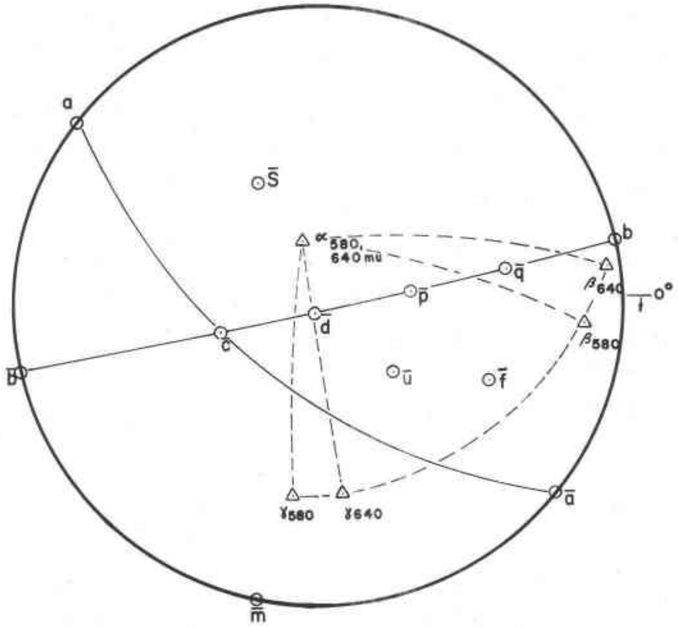

Fig. 3. Stereographic projection of a single crystal (see Table 2) and optic orientation at two wavelengths (see Table 7).

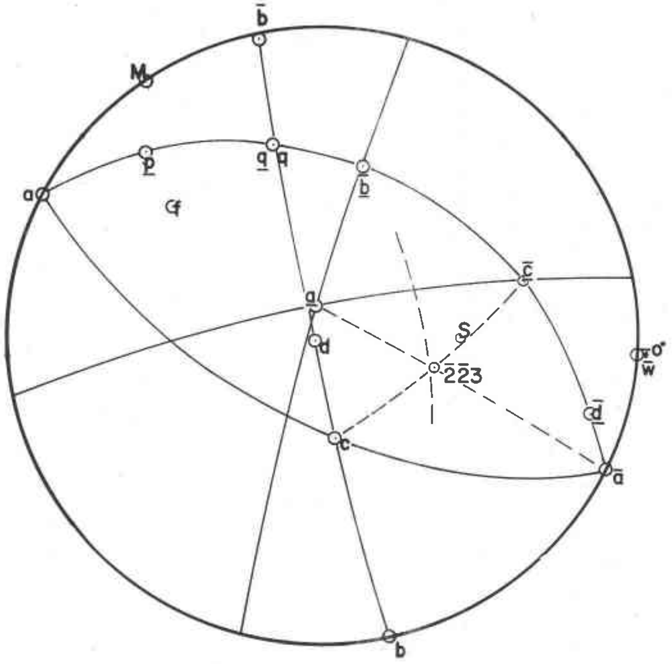

Fig. 4. Stereographic projection of twin on (2̄2̄3) from data in Table 2.

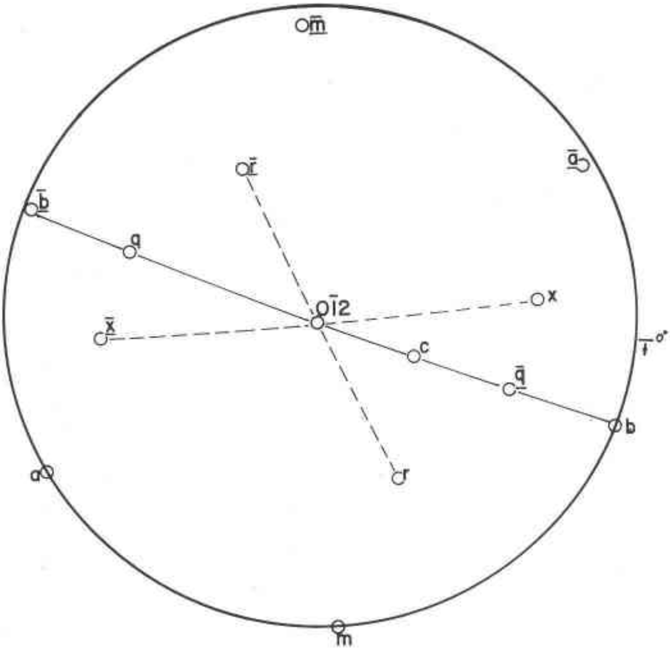

Fig. 5. Stereographic projection of twin on $(0\bar{1}2)$ from data in Table 2.

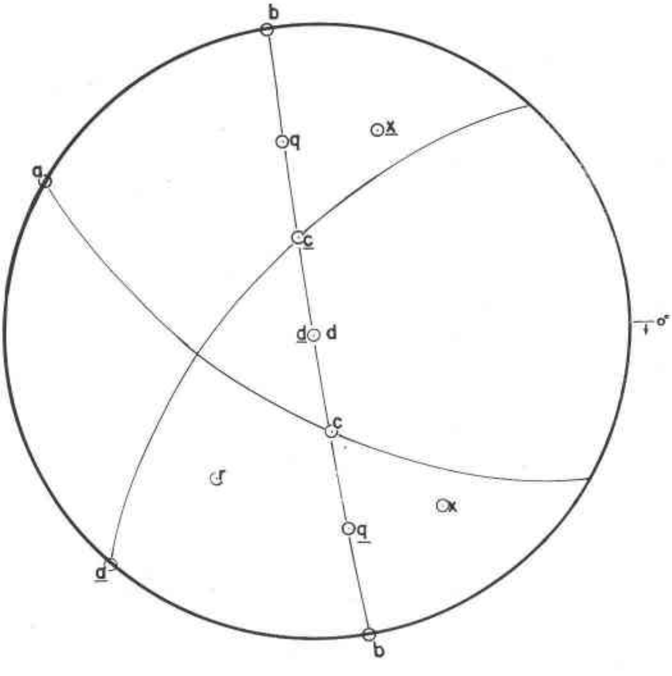

Fig. 6. Stereographic projection of twin on $(0\bar{1}0)$ from data in Table 2.

TABLE 4. UNIT-CELL CONSTANTS OF HEMIHEDRITE

	X-Ray Cell		Morphology		Delaunay Cell[b]	
	Weissenberg	Diffractometer	One Crystal[a]	Average of 42 Crystals		
a	9.497(1) Å[c]	9.495(2) Å			a'	9.954 Å
b	11.443(2)	11.441(7)			b'	10.841
c	10.841(2)	10.841(6)			c'	9.497
α	120°30(1)′	120°31(3)′	120°01′	120°16′	α'	92°06′
β	92°06(1)′	92°04(2)′	91°54′	91°54′	β'	107°58′
γ	55°50(1)′	55°53(1)′	55°51′	55°52′	γ'	123°16′
$a:b:c$	.830:.1:.947	.830:1:.948	.8345:1:.9630	.824:1:.947		
Volume 787.29 Å^3						
Density (calc.) = 6.50 g/cm^3.						

[a] From which the angle table, Table 3, was calculated.

[b] Derived from Weissenberg data. Transformation matrix morphology to Delaunay cell is $\bar{1}10/001/100$.

[c] Precisions stated are one standard deviation.

stants with morphological constants for comparison. The Delaunay reduction yields the cell given in Table 4 for which $c' < a' < b'$ with interaxial angles non-acute. The transformation matrix morphological to Delaunay cell is $\bar{1}10/001/100$. In addition to the argument presented for the morphological orientation, the retention of the cell indicated on morphological grounds is strongly supported by structural evidence. The complete structure determination (McLean and Anthony, 1970) singles out the morphological b direction as fundamental in the structure. Projections along it greatly facilitate direct comparison with other related mineral structures.

An X-ray powder pattern was prepared with Ni-filtered copper radiation (1.5418 Å) in a 114.59 mm Debye-Scherrer camera. The Straumanis mounting was used to correct for film shrinkage. The pattern yielded more than 100 measurable lines, the low theta orders of which were indexed using the cell parameters derived from Weissenberg photographs. Interplanar spacings, intensities, visually estimated with the use of a calibrated film strip, and indices are given in Table 5.

OPTICS

In thin section hemihedrite shows feeble pleochroism with $Z > Y > X$. A poor cleavage on (110) is enhanced by grinding and its trace may show extinctions of up to 30° to α in prismatic sections. Relief is extreme. Refringence data are given in Table 6.

Dispersion is noticeable in interference figures and resembles horizontal

Table 5. X-Ray Powder Data for Hemihedrite.[a] CuKα = 1.5418 Å.

I^{b}	d(obs.), Å	d(calc.), Å	hkl
4	8.765	8.755	001
3	7.481	7.366	100
9	5.512	5.508	111
3	5.384	5.416	$0\bar{1}2$
90	4.872	4.880	120
30	4.675	4.691	$\bar{1}22$
80	4.364	4.363	220
3	4.136	4.156	$1\bar{1}0$
20	3.909	3.917	201
4	3.820	3.826	020
20	3.676	3.683	200
3	3.584	3.590	$\bar{2}\bar{2}2$
30	3.478	3.477	202
20	3.399	3.404	$\bar{1}\bar{2}3$
100	3.301	3.301	$1\bar{2}2$
10	3.234	3.218	$\bar{1}\bar{3}3$
80	3.164	3.163	320
80	3.102	3.109	103
		3.095	012
2	3.033	3.038	$\bar{2}01$
10	3.019	3.023	$2\bar{1}1$
		3.012	$\bar{1}\bar{1}3$
20	2.933	3.001	$1\bar{2}3$
55	2.924	2.922	$\bar{2}\bar{3}3$
45	2.849	2.855	$\bar{2}\bar{4}2$
30	2.774	2.777	$\bar{3}\bar{3}2$
30	2.708	2.708	$0\bar{2}4$
2	2.672	2.680	$\bar{2}\bar{4}3$
		2.663	$\bar{1}\bar{4}3$
20	2.607	2.608	$\bar{3}\bar{4}2$
20	2.558	2.556	$1\bar{1}4$
30	2.514	2.519	322
10	2.450	2.448	$\bar{1}12$
		2.454	$1\bar{3}3$
10	2.420	2.421	340
20	2.354	2.356	430
30	2.324	2.326	$0\bar{4}2$
20	2.299	2.302	$1\bar{3}1$
		2.302	313
		2.299	421
10	2.244	2.245	$\bar{3}\bar{5}2$
45b[c]	2.182	2.183	411
		2.181	440
10	2.124	2.124	341
		2.120	410
20	2.077	2.078	$2\bar{2}0$
20	2.042	2.044	$1\bar{3}0$
20	2.009	2.009	$0\bar{4}5$
		2.009	$1\bar{3}5$
10	1.994	1.995	432
10	1.956	1.957	$\bar{4}\bar{1}1$
10	1.940	1.941	$1\bar{4}4$
		1.940	$2\bar{1}5$
7	1.912	1.913	040
		1.911	$2\bar{2}5$
20	1.904	1.905	$\bar{1}22$
		1.903	$\bar{3}\bar{6}3$
20	1.876	1.876	$0\bar{5}4$
3	1.841	1.841	400
		1.838	014
5	1.823	1.825	$2\bar{3}1$
		1.822	$\bar{2}21$
5	1.808	1.808	$\bar{3}\bar{5}5$
		1.808	$\bar{5}\bar{4}1$
9	1.779	1.779	$2\bar{3}5$
		1.775	542
3	1.754	1.753	$1\bar{2}6$
9	1.737	1.739	404
		1.735	$4\bar{1}2$
8	1.716	1.718	$\bar{3}\bar{6}5$
		1.714	$\bar{1}\bar{5}6$
8	1.686	1.686	$\bar{1}\bar{6}5$
		1.685	215
3	1.663	1.665	424
		1.663	$2\bar{3}0$
20	1.647	1.647	$3\bar{2}0$
		1.647	$\bar{2}04$
10	1.621	1.621	$\bar{3}03$
		1.620	$0\bar{1}6$
11	1.613		
10	1.598		
11	1.579		
5	1.566		
9	1.548		
2	1.518		
5	1.505		
5	1.494		
3	1.479		
3	1.464		
5	1.460		
9	1.425		
10	1.415		
17	1.394		
3	1.391		
10	1.373		
4	1.349		
10	1.338		
8	1.324		
6	1.316		
9	1.305		
8	1.295		
11	1.285		
10	1.274		
11	1.260		
9	1.236		
10	1.230		

[a] Indexing on basis of the morphological cell and Weissenberg data

[b] Intensity visually estimated with calibrated film strip

[c] b = broad line

Plus 28 additional lines to 0.779 Å

Table 6. Optical Constants of Hemihedrite.

$\alpha = 2.105 \pm 0.005$ yellow
$\beta = 2.32 \pm 0.02$ yellow
$\gamma = 2.65 \pm 0.02$ orange
birefringence $= 0.545$
$2V_z$(meas.) $= 92°$ (−)
$2V_z$(calc.) $= 88°$ (+)

dispersion. The optical orientation (Table 7) was determined by universal stage methods using a goniometrically oriented, right-handed crystal. The crystal is assumed to be oriented so as to give ϕ and ρ angles as shown in Table 2. A stereographic projection of the optical orientation is shown in Figure 3.

Optical activity could not be demonstrated in interference figures taken from thin sections. Attempts to see such effects in thick sections failed owing to strong scattering and absorption of incident light.

Conclusions

Hemihedrite has been carefully compared to crocoite, phoenicochrotie (Temple, 1956) and iranite (Bariand and Herpin, 1963). Powder patterns of these chromates show certain similarities (Table 8) so that confusion could arise.

A specimen of "jossaite" (Breithaupt, 1858), provided by the U.S. National Museum (cat. no. R6032) was examined and proved to be crocoite. The crystals on this specimen fit the description given by Breithaupt.

Type specimens of hemihedrite will be deposited at the U.S. National Museum and the University of Arizona.

Acknowledgments

We are grateful to Mr. R. W. Thomssen for bringing the problem to our attention and providing specimens of the type material. Mr. Thomssen kindly wrote the section on the geology of the type locality.

Mr. Richard A. Bideaux has provided help in many of the computations. The morphological angle table was computed by him.

Table 7. Optical Orientation and Its Dispersion

	ϕ 580 nm	ρ 580 nm	ϕ 640 nm	ρ 640 nm
α	−90.1°	25.7°	−90.1°	25.7°
β	163.7	82.3	175.3	88.0
γ	70.0	65.1	84.2	64.2

TABLE 8. STRONG POWDER DIFFRACTION LINES OF FOUR CHROMATES.

Crocoite USNM R-9618		Phoenicochroite (Beresov)		Iranite (Iran)		Hemihedrite (type locality)	
d(Å)	*I*	*d*(Å)	*I*	*d*(Å)	*I*	*d*(Å)	*I*
						4.87	9
						4.36	8
		3.59	5	3.60	10		
3.48	8			3.49	10	3.48	3
		3.39	10				
3.28	10			3.28	10	3.30	10
				3.18	10	3.16	8
				3.08	10	3.10	8
3.01	7	2.99	8				

Mr. John Jago provided a specimen of phoenicochroite for comparison; Mr. Pau Desautels of the U.S. National Museum provided crocoite and "jossaite." Dr. A. K. Temple provided information on phoenicochroite from Leadhills-Wanlockhead. Dr. Clifford Frondel provided a specimen of Beresov phoenicochroite. Mr. Robert B. Laughon kindly made the electron-probe examination of hemihedrite.

We are pleased to acknowledge the many assistances of Dr. W. John McLean who determined the precise unit-cell parameters and who maintained a continuing interest throughout the study.

We are grateful to Dr. A. Pabst who criticized an early version of the manuscript. Dr. J. D. H. Donnay has spent an inordinate amount of time reviewing and correcting the manuscript, and the quality of the paper owes much to his efforts.

REFERENCES

BARIAND, P., AND P. HERPIN (1963) Une nouvelle espèce minerale: Iranite, chromate hydraté de plomb. *Bull. Soc. Fr. Mineral. Cristallogr.* **86,** 133–135.

BOND, W. L. (1946) Computation of interfacial angles, interzonal angles, and clinographic projection by matrix methods. *Amer. Mineral.* **31,** 31–42.

BREITHAUPT, A. (1858) Jossaite. *Berg Huttenmannische Z.* **17,** 54–55.

DONNAY, J. D. H., G. Donnay, E. G. Cox, O. Kennard, and M. V. King (1963) *Crystal Data. Amer Crystallogr. Ass. Monogr.* **5,** 63.

EVANS, H. T., JR. (1948) Relations among crystallographic elements. *Amer. Mineral.* **33,** 60–63.

MCLEAN, W. J., AND J. W. ANTHONY (1970) The crystal structure of hemihedrite. *Amer. Mineral.* **55,** 1103–1114.

TEMPLE, A. K. (1956) The Leadhills-Wanlockhead lead and zinc deposits. *Trans. Roy. Soc., Edinburgh* **63,** 1.

WILLIAMS, S. A. (1966) The significance of habit and morphology of wulfenite. *Amer. Mineral* **51,** 1212–1217

Manuscript received, April 7, 1969; accepted for publication, April 8, 1970.